Click Here for Full Article

Physical control on the seasonal cycle of surface pCO_2 in the equatorial Pacific

Mingshun Jiang[1] and Fei Chai[2]

Received 10 June 2006; revised 31 October 2006; accepted 7 November 2006; published 9 December 2006.

[1] The controlling mechanism of the seasonal cycle of surface partial pressure of CO_2 (pCO_2) in the central/eastern equatorial Pacific is studied using a coupled physical-biogeochemical model. The model results indicate that the individual components of physical transport of total CO_2 (TCO_2) in the Niño3 area are out of phase with each other such that the net TCO_2 transport is an order smaller. This net transport is further nearly balanced by the biological drawdown and air-sea CO_2 flux combined, resulting in a weak seasonality of surface TCO_2. As a consequence, the seasonal cycle of sea surface temperature (SST) controls the surface pCO_2 cycle with a maximum in boreal spring-summer and a minimum in boreal fall-winter. In turn, the seasonality of air-sea CO_2 flux is largely controlled by SST and surface winds via the piston velocity of gas exchange. Perturbations to the subtle balance of TCO_2 transport by dynamical processes on other timescales such as El Niño, La Niña and tropical instability waves, could induce significant change to the surface pCO_2, in addition to the change due to SST variability. **Citation:** Jiang, M. S., and F. Chai (2006), Physical control on the seasonal cycle of surface pCO_2 in the equatorial Pacific, *Geophys. Res. Lett.*, *33*, L23608, doi:10.1029/2006GL027195.

1. Introduction

[2] The equatorial Pacific represents the largest oceanic source of CO_2 to the atmosphere due to its vast area and high partial pressure of CO_2 (pCO_2) in the surface layer [e.g., *Tans et al.*, 1990; *Takahashi et al.*, 1997, 2002]. Persistent upwelling of the CO_2-rich subsurface water into the surface layer and the relatively slow air-sea exchange as compared to upwelling [*Feely et al.*, 1987; *Wanninkhof et al.*, 1995; *Chavez et al.*, 1999] lead to excessive CO_2, hence high pCO_2 in the surface layer over the entire basin. Surface pCO_2 in the equatorial Pacific undergoes a significant seasonal cycle with a maximum in boreal spring-summer and a minimum in boreal fall-winter [*Takahashi et al.*, 1997, 2002; *Feely et al.*, 2002, 2004, 2006; *Cosca et al.*, 2003]. Since equatorial upwelling is driving the seasonal change of surface total CO_2(TCO_2) [e.g., *Wanninkhof et al.*, 1995; *Feely et al.*, 2002; *Wang et al.*, 2006], it is puzzling that the pCO_2 cycle is out of phase with the upwelling, which is strongest in winter and weakest in spring [*Meinen et al.*, 2001]. *Cosca et al.* [2003] suggested that relatively elevated biological activity in fall might have offset the upwelling of TCO_2 and caused the relatively low surface pCO_2 in fall-winter. Recently *Wang et al.* [2006] suggested that surface pCO_2 was relatively high in both spring and fall, and that surface TCO_2 dominated the seasonal cycle of pCO_2 except for the SST-induced spring peak. *Wang et al.* [2006] further suggested significant modulation of biological activity to surface TCO_2 but did not estimate the contribution of biological export to the season variation of surface pCO_2. Earlier modeling efforts have over-estimated the biological export by 3 to 4 times as compared to the observed export production [*Winguth et al.*, 1994; *Le Quéré et al.*, 2000; *Obata and Kitamura*, 2003].

[3] In this communication, the mechanism of surface pCO_2 seasonal cycle in the equatorial Pacific is investigated using a coupled physical-biogeochemical model driven by monthly climatological forcing [*Jiang et al.*, 2003; *Jiang and Chai*, 2005]. The contribution of biological export to the pCO_2 seasonal variation is also examined. We will focus on the Niño3 area (5°N–5°S, 150°W–90°W) where the largest seasonal variation of surface pCO_2 in the equatorial Pacific is detected [e.g., *Takahashi et al.*, 2002; *Feely et al.*, 2002; *Cosca et al.*, 2003].

2. Model Description and Numerical Experiments

[4] The numerical model is a coupled physical-biogeochemical model for the Pacific Ocean [*Chai et al.*, 2003; *Jiang et al.*, 2003]. The physical model is the NCAR climate ocean model (NCOM) [*Li et al.*, 2001], and the biogeochemical model is based on the one-dimensional model developed by *Chai et al.* [2002]. Carbon cycle is simulated with a fixed Redfield C/N ratio and air-sea CO_2 flux is determined by the product of the air-sea pCO_2 difference and the piston velocity of gas exchange [*Wanninkhof*, 1992]. The calculation of sea surface pCO_2 follows *Peng et al.* [1987] with the alkalinity linearly linked to normalized salinity [*Millero et al.*, 1998].

[5] The coupled model is initialized with climatological temperature and salinity [*Levitus et al.*, 1994; *Levitus and Boyer*, 1994], nutrients [*Conkright et al.*, 1998], and TCO_2 [*Key et al.*, 2004]. The model is forced with the monthly means of 47-yr (1946–1993) heat fluxes and wind stresses from the Comprehensive Ocean Analysis Data Set (COADS) [*Li et al.*, 2001] and the atmospheric pCO_2 observed at Mauna Loa in 1990 [e.g., *Keeling et al.*, 1996]. More details can be found in work by *Jiang et al.* [2003] and *Jiang and Chai* [2005].

[6] Three numerical experiments were conducted to delineate the effects of temperature and biological production on the pCO_2 seasonal cycle. In the control experiment (CTRL), the seasonal cycles of both physics and biology were fully resolved. In the second experiment (FixNP), new

[1]Environmental Coastal Ocean Sciences, University of Massachusetts-Boston, Boston, Massachusetts, USA.
[2]School of Marine Sciences, University of Maine, Orono, Maine, USA.

Copyright 2006 by the American Geophysical Union.
0094-8276/06/2006GL027195$05.00

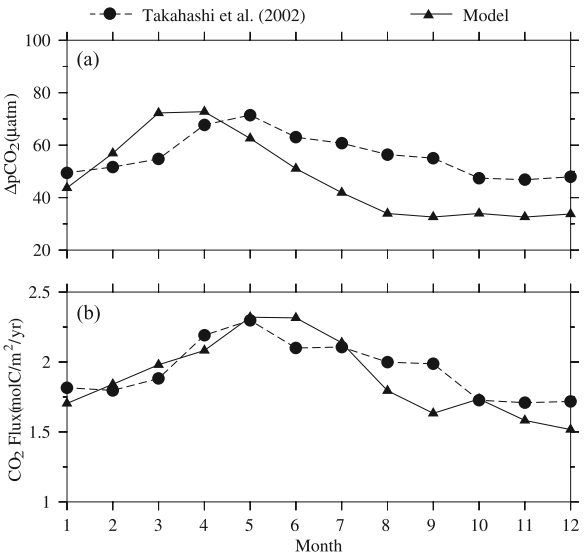

Figure 1. (a) Model and observed surface ΔpCO_2 in the Niño3 area. (b) Model and observed air-to-sea CO_2 flux. Data were from *Takahashi et al.* [2002].

and export production at each grid points were set to their annual mean values derived from the CTRL experiment, while the other processes were kept unchanged. In the third experiment (FixSST), surface pCO_2 in the CTRL experiment was re-calculated with the annual mean field of SST.

3. Results and Discussion

[7] The average ΔpCO_2 (pCO_2 at sea surface minus pCO_2 in the atmosphere) in the Niño3 area from the CTRL experiment is compared with the climatological mean ΔpCO_2 (Figure 1a) [*Takahashi et al.*, 2002]. Both modeled and observed surface ΔpCO_2 show a strong seasonal cycle with a distinct peak in boreal spring (March–May) and a low in the boreal fall-winter period, though the modeled peak is about one month earlier. Modeled ΔpCO_2 shows a seasonal variation of 40 μatm, which is larger than that projected by *Takahashi et al.* [2002]. However, modeled seasonal variation is within the observed range of 20–50 μatm in the area of 125°W–95°W from underway measurements during 1992–2001 [*Cosca et al.*, 2003]. In central equatorial Pacific, the model predicts a small seasonal variation about 10 μatm, which is consistent with the synthesis results from underway measurements by *Feely et al.* [2002] and *Cosca et al.* [2003] but is lower than the seasonal variation projected by *Takahashi et al.* [2002]. The annual mean pattern of modeled surface ΔpCO_2 compares well with the climatological projection, but modeled values are about 20 μatm lower in central and eastern equatorial Pacific [*Jiang and Chai*, 2005].

[8] As the product of ΔpCO_2 and the piston velocity of gas exchange, modeled air-sea CO_2 flux in the Niño3 area peaks in June (Figure 1b), in agreement with the climatological projection by *Takahashi et al.* [2002], which used NCEP/NCAR monthly mean wind speed in the calculation of the piston velocity. The reason that in fall model CO_2 flux agrees with data while model pCO_2 differs might be due to the different wind products used. Although the average COADS and NCEP wind speeds in Niño3 agree well with each other in their seasonal cycles (not shown), their spatial patterns differ and the COADS winds have a much weaker zonal component and produce more realistic thermocline in a circulation model [*Wu and Xie*, 2003]. The impact of these differences on the CO_2 flux estimate is not immediately clear without a detailed comparison because of the nonlinear dependence of piston velocity on wind speed. It is also possible that the coarse grid (4° × 5°) used in the projection over-smoothed the seasonal cycle of ΔpCO_2. Modeled total CO_2 flux in the tropical Pacific (14°N–14°S) is approximately 0.8 GtC yr^{-1}, similar to the climatological projection of 0.73–0.78 GtC yr^{-1} [*Takahashi et al.*, 2002] and the model result of 0.6 GtC yr^{-1} by *Wang et al.* [2006].

[9] Surface pCO_2 is largely determined by surface TCO_2 concentration and SST. The temporal change of TCO_2 in the surface layer is determined by the net physical transport including mixing, air-sea CO_2 exchange, and biological export. A budget analysis for the Niño3 box (5°N–5°S, 150°W–90°W, 0–50 m) in the CTRL experiment indicates that horizontal advection of TCO_2 nearly balances the upwelling flux (~270 mol m^{-2} yr^{-1}), which results in a much smaller net TCO_2 transport (Table 1 and Figure 2). The upwelling flux of TCO_2 at 50 m is largely controlled by the upwelling velocity, because TCO_2 concentration at 50 m has a small seasonal change with a maximum in March due to the upward shoaling of the thermocline [see, e.g., *Philander*, 1990]. Model upwelling velocity at 50 m is largest in winter and smallest in summer, consistent with the estimates from the TOGA buoy measurements [*Meinen et al.*, 2001]. The upwelling and net meridional fluxes are generally in-phase each other, but much larger than and out-of-phase with the net zonal flux. The meridional flux at 5°N is northward ranging from 7 to 12 GtC yr^{-1} in winter-spring months, while it is much smaller during the rest of the year and switches to southward in summer. The meridional flux at 5°S is persistently southward with a range of 8 to 15 GtC yr^{-1} and a peak in summer. As a result of these phase differences, the net transport of TCO_2 has a maximum in March–April and a minimum in August–September, although the upwelling flux has a maximum in winter and a minimum in summer. On the other hand, the timescale of surface CO_2 reaching equilibrium with the atmosphere is about half a year [*Broecker and Peng*, 1982], and as a result, surface TCO_2 is lagging about 3 to 4 months behind the net transport. In other words, it is the net physical transport of TCO_2, rather than the upwelling itself, that dominates in the seasonal cycle of surface TCO_2.

Table 1. TCO_2 Budget for the Niño3 Box (5°N–5°S, 150°W–90°W, 0–50 m)[a]

Fluxes	Values, GtC yr^{-1}
Upwelling flux at 50 m	22.8 (±4.7)
Net zonal flux	−5.4 (±2.8)
Net meridional flux	−17.0 (±4.1)
Net transport	0.39 (±0.16)
Biological export	−0.25 (±0.03)
Air-sea exchange	−0.19 (±0.02)

[a]Numbers in the parentheses are the standard deviations of these fluxes. A negative value indicates an outgoing flux.

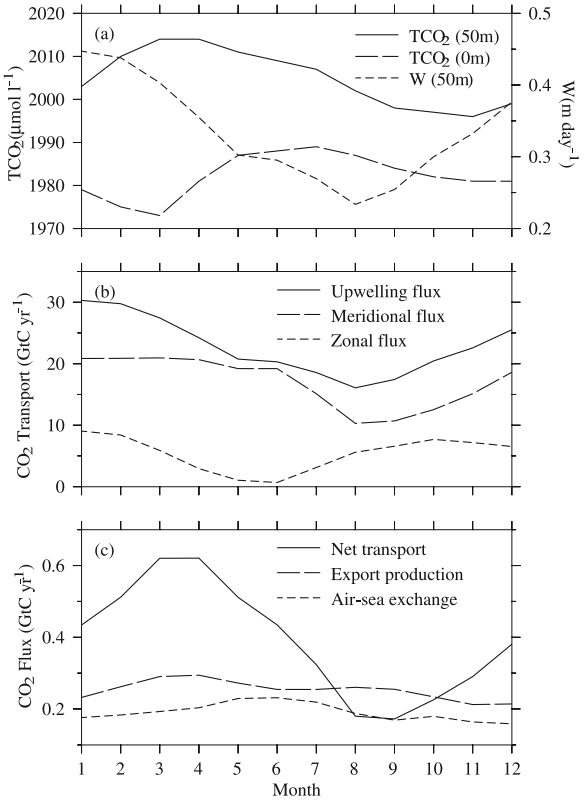

Figure 2. (a) TCO_2 concentrations and vertical velocity in the Niño3 area. (b) Upwelling and horizontal transport of TCO_2 for the Niño3 box (5°N–5°S, 150°W–90°W, 0–50 m) (both the zonal and meridional fluxes are out of the box). (c) Net carbon transport, carbon export by biological production, and air-sea exchange for the Niño3 box (both biological export and air-sea exchange are out of the box).

[10] The carbon budget analysis also indicates that the air-sea CO_2 flux and biological drawdown of CO_2 play a small role in the seasonal cycle of surface TCO_2 in the Niño3 area. Both the air-sea CO_2 flux and biological export have small seasonal variations as compared to the net TCO_2 transport. However, the sum of annual mean air-sea exchange (2.1 mol m^{-2} yr^{-1}) and biological export (2.9 mol m^{-2} yr^{-1}) nearly balances the net physical transport (Figure 2c). Both the biological export and primary production (not shown) have a maximum in March–April and a secondary peak in August–September, consistent with the climatological mean primary production measured in 1983–1996 (R.T. Barber, personal communication, 2001) and the modeled export by *Wang et al.* [2006]. The overall values of modeled primary production and export production agree with historical observations quite well, see *Jiang et al.* [2003] for a detailed comparison. A weak seasonal variation of primary production simulated is consistent with the weak seasonal variations of modeled and observed primary production in 1992 [*Chavez et al.*, 1996; *Wang et al.*, 2006], even though a moderate El Niño event occurred in spring 1992. The increased production in spring is due to the elevated nutrient concentrations (not shown) and increased water temperature induced by the upward shoaling of the thermocline. In fall-winter, the much deeper surface mixed layer [see, e.g., *Wang et al.*, 2006] offsets the strong upwelling and leads to the relatively low surface nutrient concentrations.

[11] A weak seasonal cycle of surface TCO_2 in the Niño3 area leaves the control of surface pCO_2 seasonal cycle to the SST. Model SST generally agrees with observed SST [*Reynolds et al.*, 2002] and both are high in spring and low in fall-winter in response to the variability of trade winds [*Philander*, 1990] (Figure 3). Without the seasonal variation of SST (FixSST experiment), the modeled surface pCO_2 in the Niño3 area has an average of 50 μatm (the same as that in the CTRL experiment) and a seasonal change of about 12 μatm with a small peak in fall, when the atmospheric pCO_2 and surface TCO_2 also reach their maxima (Figure 3). As a result, the ΔpCO_2 anomaly between the CTRL and FixSST experiments accounts for more than 80% of the pCO_2 variation over the year. In turn, the seasonal cycle of air-sea CO_2 flux is controlled by SST and surface winds while biological activity and physical transport play small roles in this process. These results are significantly different from the model results by *Wang et al.* [2006], which predicted similar spatial and temporal pattern of surface TCO_2 and pCO_2 with two peaks (spring and fall) and a fall-winter maximum of air-sea CO_2 flux. *Wang et al.* [2006] further suggested that surface TCO_2 dominated the seasonal cycle of pCO_2 with additional warming effect in spring. However, an under-estimated seasonal variation of SST in their model (about 1°C as compared to our 2°C and observed 3°C, see Figure 3b) may have led to an under-estimation of temperature effect on surface pCO_2 cycle.

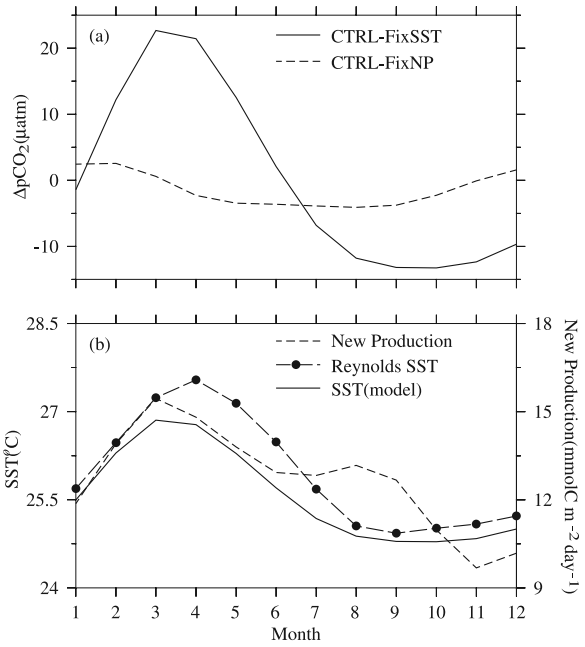

Figure 3. (a) Surface ΔpCO_2 differences between the CTRL and FixSST experiments, and the differences between the CTRL and FixNP experiments in the Niño3 area. (b) Model SST, Reynolds SST [*Reynolds et al.*, 2002], and model new production in the Niño3 area.

[12] The biological drawdown contributes about 6 μatm to the seasonal variation of surface pCO_2 as can be seen from the pCO_2 differences between the CTRL and FixNP experiments (Figure 3). In the FixNP experiment, the new production in spring is smaller than in the CTRL experiment, which leads to the accumulation of surface TCO_2 and hence increases surface pCO_2 in summer. By contrast, higher new production in the FixNP experiment during fall and winter leads to reduced surface TCO_2 in winter.

[13] The subtle balance of CO_2 transport and dominance of the net physical transport on the seasonal surface TCO_2 budget in the Niño3 area have significant implications for the pCO_2 variability in other timescales such as intra-seasonal and inter-annual variability. Different from the dominance of upwelling on the nutrient budget in the surface layer of the equatorial Pacific [*Toggweiler and Carson*, 1995; *Chai et al.*, 1996; *Jiang et al.*, 2003], both the meridional and zonal fluxes of TCO_2 have comparable magnitudes as the upwelling flux in this area. Therefore, the phase differences between each physical component of any perturbations to the seasonal cycle would have dramatic consequences to surface TCO_2 and likely change the SST dominance on the surface pCO_2 variability. For example, the frequent tropical instability waves (TIWs) at around 2°N would bring nutrient-poor water from the subtropical north Pacific into the equator [*Eldin and Rodier*, 2003] and hence reduce the normally northward meridional flux of TCO_2 at 5°N. Recently, *Le Borgne et al.* [2002] pointed out that the surface area of high nutrients and low chlorophyll (HNLC) in the equatorial Pacific (calculated within 1°N–1°S) has a small difference between El Niños and other periods (the area ratio of El Niño/(other years) equals 0.67). This is dramatically different from the area difference for CO_2 evasion estimated by *Feely et al.* [2002] (the area ratio equals 0.25), indicating different controls on the inter-annual variability of nitrate and TCO_2 in the equatorial Pacific. Recent observation and modeling studies have demonstrated the dominance of physical forcing on the inter-annual variability of the surface TCO_2, but the focus is largely on the changes of the upwelling and zonal fluxes [e.g., *Chavez et al.*, 1999; *Le Quéré et al.*, 2000; *Feely et al.*, 2002; *Obata and Kitamura*, 2003]. More quantitative studies on the variability of meridional flux (and related processes such as TIWs) are needed given its large value and significant seasonal variation.

[14] **Acknowledgments.** This research was supported by NASA and NSF grants to F. Chai. We thank T. Takahashi for sharing pCO_2 and CO_2 flux data and some useful discussion. Two anonymous reviewers provided constructive comments that greatly improved the manuscript.

References

Broecker, W. S., and T.-H. Peng (1982), *Tracers in the Sea*, 690 pp., Lamont-Doherty Earth Obs., Palisades, N. Y.

Chai, F., et al. (1996), Origin and maintenance of a high nitrate condition in the equatorial Pacific, *Deep Sea Res., Part II*, *43*, 1031–1064.

Chai, F., et al. (2002), One dimensional ecosystem model of the equatorial Pacific upwelling system, part I: Model development and silicon and nitrogen cycle, *Deep Sea Res., Part II*, *49*, 2713–2745.

Chai, F., et al. (2003), Interdecadal variation of the transition zone chlorophyll front: A physical-biological model simulation between 1960 and 1990, *J. Oceanogr.*, *59*(4), 461–475.

Chavez, F. P., et al. (1996), Phytoplankton variability in the central and eastern tropical Pacific, *Deep Sea Res., Part II*, *43*, 835–870.

Chavez, F. P., et al. (1999), Biological and chemical response of the equatorial Pacific Ocean to the 1997–98 El Niño, *Science*, *286*, 2126–2131.

Conkright, M. E., et al. (1998), *World Ocean Database 1998*, CD-ROM data set documentation, *Natl. Oceanogr. Data Cent. Internal Rep. 14*, 111 pp., NOAA, Silver Spring, Md.

Cosca, C. E., R. A. Feely, J. Boutin, J. Etcheto, M. J. McPhaden, F. P. Chavez, and P. G. Strutton (2003), Seasonal and interannual CO_2 fluxes for the central and eastern equatorial Pacific Ocean as determined from fCO_2-SST relationships, *J. Geophys. Res.*, *108*(C8), 3278, doi:10.1029/2000JC000677.

Eldin, G., and M. Rodier (2003), Ocean physics and nutrient fields along 180° during an El Niño–Southern Oscillation cold phase, *J. Geophys. Res.*, *108*(C12), 8137, doi:10.1029/2000JC000746.

Feely, R. A., R. H. Gammon, B. A. Taft, P. E. Pullen, L. S. Waterman, T. J. Conway, J. F. Gendron, and D. P. Wisegarver (1987), Distributions of chemical tracers in the eastern equatorial Pacific during and after the 1982–1983 El Niño/Southern Oscillation event, *J. Geophys. Res.*, *92*(C6), 6545–6558.

Feely, R. A., et al. (2002), Seasonal and interannual variability of CO_2 in the equatorial Pacific, *Deep Sea Res., Part II*, *49*, 2443–2469.

Feely, R. A., R. Wanninkhof, W. McGillis, M.-E. Carr, and C. E. Cosca (2004), Effects of wind speed and gas exchange parameterizations on the air-sea CO_2 fluxes in the equatorial Pacific Ocean, *J. Geophys. Res.*, *109*, C08S03, doi:10.1029/2003JC001896.

Feely, R. A., T. Takahashi, R. Wanninkhof, M. J. McPhaden, C. E. Cosca, S. C. Sutherland, and M.-E. Carr (2006), Decadal variability of the air-sea CO_2 fluxes in the equatorial Pacific Ocean, *J. Geophys. Res.*, *111*, C08S90, doi:10.1029/2005JC003129.

Jiang, M. S., and F. Chai (2005), Physical and biological controls on the latitudinal asymmetry of surface nutrients and pCO_2 in the central and eastern equatorial Pacific, *J. Geophys. Res.*, *110*, C06007, doi:10.1029/2004JC002715.

Jiang, M. S., et al. (2003), A nitrate and silicate budget in the equatorial Pacific Ocean: A coupled physical-biological model study, *Deep Sea Res., Part II*, *50*, 2971–2996.

Keeling, C. D., et al. (1996), Increased activity of northern vegetation inferred from atmospheric CO_2 measurements, *Nature*, *382*, 146–149.

Key, R. M., A. Kozyr, C. L. Sabine, K. Lee, R. Wanninkhof, J. L. Bullister, R. A. Feely, F. J. Millero, C. Mordy, and T.-H. Peng (2004), A global ocean carbon climatology: Results from Global Data Analysis Project (GLODAP), *Global Biogeochem. Cycles*, *18*, GB4031, doi:10.1029/2004GB002247.

Le Borgne, R., et al. (2002), Carbon fluxes in the equatorial Pacific: A synthesis of the JGOFS programme, *Deep Sea Res., Part II*, *49*, 2425–2442.

Le Quéré, C., J. C. Orr, P. Monfray, and O. Aumont (2000), Interannual variability of the oceanic sinks of CO_2 from 1979 to 1997, *Global Biogeochem. Cycles*, *14*, 1247–1265.

Levitus, S., and T. P. Boyer (1994), *World Ocean Atlas 1994*, vol. 4, *Temperature*, *NOAA Atlas NEDIS 4*, NOAA, Silver Spring, Md.

Levitus, S., R. Burgett, and T. P. Boyer (1994), *World Ocean Atlas 1994*, vol. 3, *Salinity*, *NOAA Atlas NEDIS 3*, NOAA, Silver Spring, Md.

Li, X. J., et al. (2001), A comparison of two vertical mixing schema in a Pacific Ocean general model, *J. Clim.*, *14*, 1377–1398.

Meinen, C. S., et al. (2001), Vertical velocities and transports in the equatorial Pacific during 1993–99, *J. Phys. Oceanogr.*, *31*(11), 3230–3248.

Millero, F. J., et al. (1998), Distribution of alkalinity in the surface waters of the major oceans, *Mar. Chem.*, *60*(1–2), 111–130.

Obata, A., and Y. Kitamura (2003), Interannual variability of the sea-air exchange of CO_2 from 1961 to 1998 simulated with a global ocean circulation-biogeochemistry model, *J. Geophys. Res.*, *108*(C11), 3337, doi:10.1029/2001JC001088.

Peng, T. H., et al. (1987), Seasonal variability of carbon dioxide, nutrients and oxygen in the northern North Atlantic surface water: Observations and model, *Tellus, Ser. B*, *39*, 439–458.

Philander, S. G. (1990), *El Niño, La Niña, and the Southern Oscillation*, 288 pp., Elsevier, New York.

Reynolds, R. W., et al. (2002), An improved in situ and satellite SST analysis for climate, *J. Clim.*, *15*, 1609–1625.

Takahashi, T., et al. (1997), Global air-sea flux of CO_2: An estimate based on measurements of sea-air pCO_2 difference, *Proc. Natl. Acad. Sci. U. S. A.*, *94*, 8292–8299.

Takahashi, T., et al. (2002), Global sea-air CO_2 flux based on climatological surface ocean pCO_2, and seasonal biological and temperature effects, *Deep Sea Res., Part II*, *49*, 1601–1622.

Tans, P. P., et al. (1990), Observational constraints on the global atmospheric CO_2 budget, *Science*, *247*, 1431–1438.

Toggweiler, J. R., and S. Carson (1995), What are the upwelling systems contributing to the Ocean's carbon and nutrient budgets, in *Upwelling in the Ocean: Modern Processes and Ancient Records*, *Environ. Sci. Res. Rep.*, vol. 18, edited by C. P. Summerhayes, pp. 337–360, John Wiley, Hoboken, N. J.

Wang, X., J. R. Christian, R. Murtugudde, and A. J. Busalacchi (2006), Spatial and temporal variability of the surface water pCO_2 and air-sea

CO_2 flux in the equatorial Pacific during 1980–2003: A basin-scale carbon cycle model, *J. Geophys. Res.*, *111*, C07S04, doi:10.1029/2005JC002972.

Wanninkhof, R. (1992), Relationship between wind speed and gas exchange over the ocean, *J. Geophys. Res.*, *97*, 7373–7378.

Wanninkhof, R., et al. (1995), Seasonal and lateral variations in carbon chemistry of surface water in the eastern equatorial Pacific during 1992, *Deep Sea Res., Part II*, *42*, 387–409.

Winguth, A. M. E., M. Heimann, K. D. Kurz, E. Maier-Reimer, U. Mikolajewicz, and J. Segschneider (1994), El Niño–Southern Oscillation related fluctuations of the marine carbon cycle, *Global Biogeochem. Cycles*, *8*, 39–64.

Wu, R., and S.-P. Xie (2003), On equatorial Pacific surface wind changes around 1977: NCEP-NCAR reanalysis versus COADS observations, *J. Clim.*, *6*, 167–173.

F. Chai, School of Marine Sciences, University of Maine, Orono, ME 04469, USA. (fchai@maine.edu)

M. S. Jiang, Environmental Coastal Ocean Sciences, University of Massachusetts-Boston, 100 Morrissey Blvd., Boston, MA 02125, USA. (mingshun.jiang@umb.edu)